

유연송전시스템에서의 역률 보상을 위한 배전용 정지형 동기조상기의 전류제어

오관일^o, 문건우, 전영수, 이기선, 추진부
한전전력연구원 전력계통연구실 차세대전력전송그룹

Predictive Current Control of Distribution Static Condenser (D-STATCON) for Reactive Power Compensation in Flexible AC Transmission System(FACTS)

Kwan-IL Oh^o, Gun-Woo Moon, Young-Soo Jeon, Ki-Sun Lee, Jin-Boo Choo
FACTS Group Electrical System Research Lab. KEPRI

Abstract

This paper describes a modeling and current control techniques of Distribution static condenser (D-STATCON) for power factor compensation. The current control is based on the predictive and the space vector PWM scheme. The predictive current controlled PWM D-STATCON can maintain its performance with power factor compensation and fixed switching frequency. By using the space vector control low ripple and offset in the current and the voltage as well as fast dynamic responses are achieved with a small DC link capacitance employed.

I. INTRODUCTION

Static var compensators(SVCs) were developed in the late 1960s to provide fast power factor compensation for large, fluctuating industrial loads, such as electric arc furnaces. These compensators used either thyristor-switched capacitors (TSCs) or a thyristor-controlled reactor (TCR) with fixed power factor correcting capacitors, which also provided, when combined with appropriate tuning reactors, harmonics filtering. In the late 1970s the

need for dynamic compensation of electric power transmission system, to achieve better utilization of existing generation and transmission facilities, had become increasingly evident. Static var compensator schemes, using TCRs in combination with TSCs and fixed capacitive filters on the secondary side of a coupling transformer, were devised and successfully applied for the dynamic compensation of power systems to provide voltage support, increase transient stability, and improve damping[1-6].

The application of modern semiconductor device, power converter circuit and control

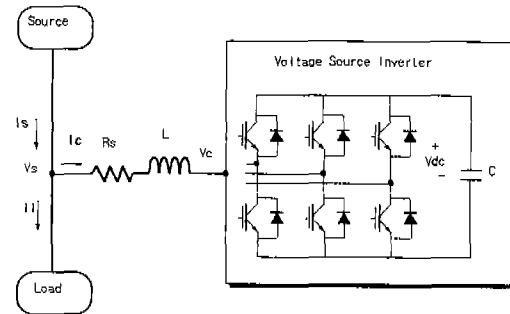


Fig. 1 Circuit Diagram of D-STATCON

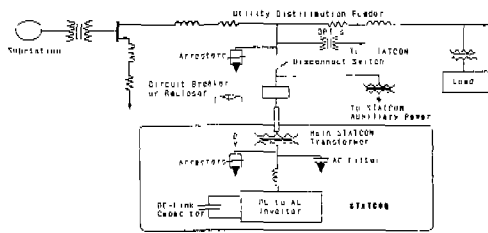


Fig. 2 Typical system interconnection

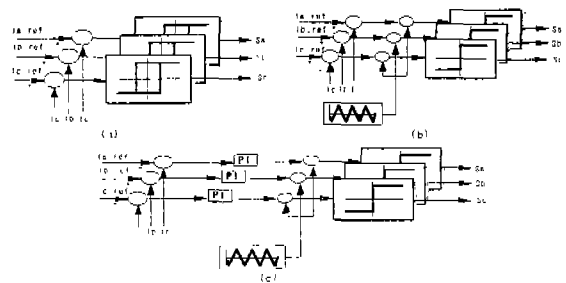


Fig. 5 Simple block diagram of the various current control technique: (a) hysteresis; (b) ramp comparison; (c) PI with ramp comparison

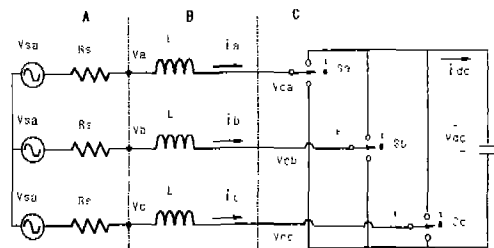


Fig. 3 Simplified main circuit of D-STATCON

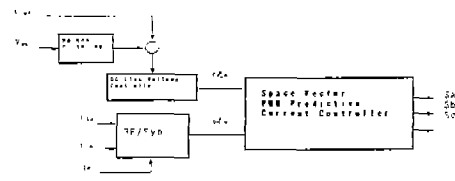


Fig. 6 Simple block diagram of space vector predictive current control

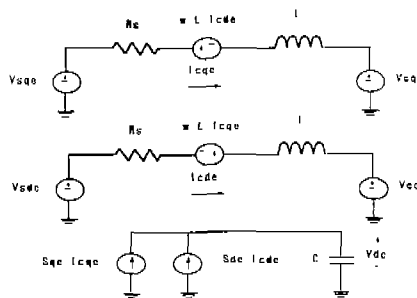


Fig. 4 Synchronous reference frame dq modeling

technologies have resulted in a solid-state var source of fundamentally different operating and functional characteristics than those obtained previously with conventional static var compensator. Since the solid-state converter approach considered in this paper can be represented as an ac voltage source behind a small coupling reactance, its V-I characteristic is similar to that of the rotating synchronous condenser and, for this reason, it is called a static condenser (STATCON) or static compensator (STATCOM) [1].

The possibility of generating controllable reactive power by various power electronic switching converter has long been realized with the use of gate turn-off(GTO) thyristors [7]. Further extensive development efforts in the areas of high power GTO valves and inverter topologies, together with advanced control technique were carried out. These technologies are widely applied to 1-100MVA system. However, the high switching frequency pulse-width modulation(PWM) operation is not available in GTO thyristor based STATCON. The switching frequency of GTO may not exceed several hundred hertz in high-power range. Recently, in order to reduce the harmonic contents of inverter output current, a number of researches on the three-level inverter have been done. However, this method is also needed bulky harmonic filters due to low switching frequency PWM operation and the snubber design is very difficult.

In the 1980s, there were dramatic advances in insulated-gate bipolar transistors (IGBT) development and the voltage and current ratings

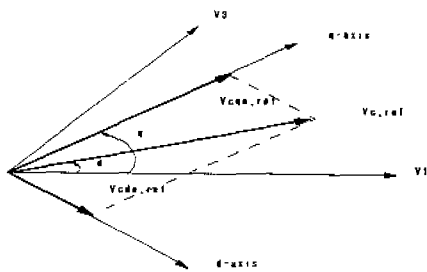


Fig. 7 Computation example of space vector PWM

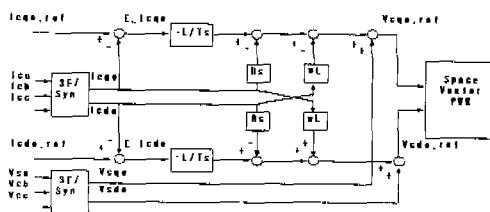


Fig. 8 Overall block diagram of predictive current controller

of the available devices rapidly increased. To demonstrate the practical feasibility of a new generation of reactive power compensators using IGBT, an experimental 1MVA installation employing devices with a voltage rating of 1200 volts and current rating of 400 amperes and 3kHz switching frequency PWM operation is reported.

In order to regulate and stabilize transmission system and to compensate industrial reactive loads, the line current must be controlled. Therefore, it forms an important task to design a PWM current controller. Many task of current control can be accomplished through the use of any number of existing current control schemes for use in voltage source inverters [8-11]. These include hysteresis controls and synchronous reference frame control, which use a proportional-integral (PI) controller and sine-triangle PWM.

This paper presents the D-STATCON using IGBT voltage source inverter with 3kHz switching frequency PWM operation for 1MVA power factor compensation in distribution system. A synchronous frame DQ modeling of D-STATCON

is presented and the various conventional and space vector predictive PWM current controls are developed. Direct control of current space vectors has the advantages of improved harmonic performance, and improved transient performance at any operating condition, in comparison to per-phase PWM techniques such as hysteresis, ramp comparison and PI with ramp current controller.

II. D-STATCON OVERVIEW AND MODELING

The 1MVA-class D-STATCON has been developed by KEPRI for advanced distribution. The D-STATCON is a solid-state dc to ac switching power converter that consist of a three-phase, voltage-sourced forced air-cooled inverter. Fig. 1 shows the basic STATCON scheme with an elementary six-pulse voltage-sourced inverter and one IGBT switch represent the series connected eight IGBT switches. In this basic form, the D-STATCON injects a voltage in phase with the system voltage, thus providing voltage support and regulation of VAR flow. Because the device generates a synchronous waveform, it is capable of generating continuously variable reactive or capacitive shunt compensation at a level of the maximum MVA rating of the D-STATCON inverter. Connection to the distribution network is via a standard distribution transformer thereby allowing the D-STATCON to be applied to all classes of distribution voltages. At the point of connection, the D-STATCON will, within the limits of its inverter, provide a highly regulated stable terminal voltage. The D-STATCON is available in ratings from 2 to 10MVA in modular 1-MVA increments. The power electronics equipment, coupling transformer and disconnecting switchgear is available in indoor lineup or outdoor pad-mount design. Further portable trailer enclosure is available. Fig. 2 shows the typical system interconnection diagram and installation point.

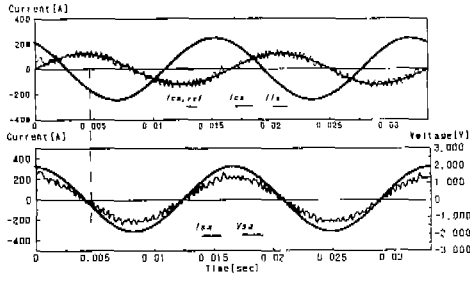


Fig. 9 Simulation results of hysteresis current control

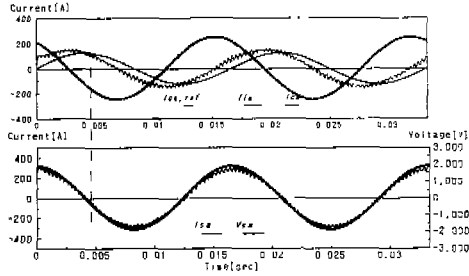


Fig. 10 Simulation results of ramp comparison current control

It is assumed the source is a balanced, sinusoidal three phase voltage supply with frequency ω . Since power factor compensation is desired, it is convenient for this analysis to take the angle of the a-phase input voltage as reference angle. That is,

$$\begin{aligned} V_{sa} &= V_m \cos \omega t \\ V_{sb} &= V_m \cos(\omega t - 2\pi/3) \\ V_{sc} &= V_m \cos(\omega t + 2\pi/3) \end{aligned} \quad (1)$$

The simplified main circuit of D-STATCON is shown in Fig. 3. By using circuit DQ transformation method [12], synchronous reference frame modeling is shown in Fig. 4, and can be obtained as follows:

$$\begin{aligned} \begin{bmatrix} \frac{di_{qe}}{dt} \\ \frac{di_{de}}{dt} \\ \frac{dV_{dc}}{dt} \end{bmatrix} &= \begin{bmatrix} -R_s/L & -\omega & 0 \\ \omega & -R_s/L & 0 \\ 0 & 0 & -1/CR_L \end{bmatrix} \begin{bmatrix} i_{qe} \\ i_{de} \\ V_{dc} \end{bmatrix} \\ &+ \frac{1}{L} \begin{bmatrix} 1 & 0 \\ 0 & 1 \\ 0 & 0 \end{bmatrix} \begin{bmatrix} V_{Sqe} \\ V_{Sde} \end{bmatrix} + \begin{bmatrix} -\frac{1}{L} V_{dc} & 0 \\ 0 & -\frac{1}{L} V_{dc} \\ \frac{1}{C} i_{qe} & \frac{1}{C} i_{de} \end{bmatrix} \begin{bmatrix} S_{qe} \\ S_{de} \end{bmatrix} \end{aligned} \quad (2)$$

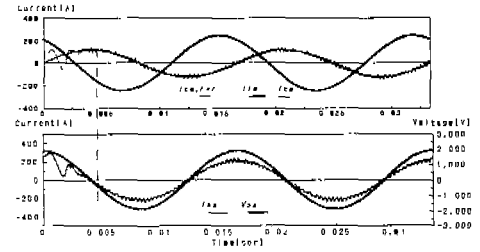


Fig. 11 Simulation results of PI with ramp comparison current control

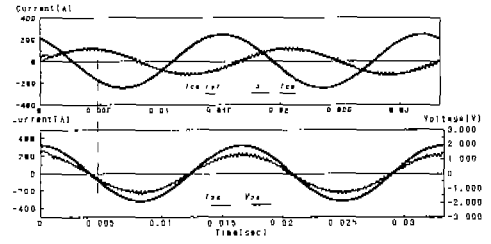


Fig. 12 Simulation results of predictive current control

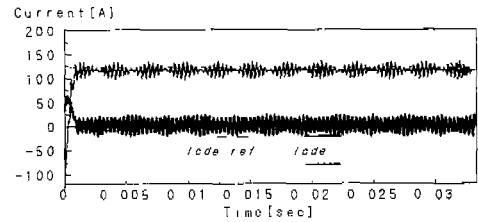


Fig. 13 DQ current reference and current of predictive current control

where i_{qe} , i_{de} , V_{Sqe} , and V_{Sde} are DQ transformed currents and source voltages, respectively. And S_{qe} and S_{de} represent DQ transformed switching function.

III. CURRENT CONTROL TECHNIQUES OF D-STATCON

In this section, a space vector predictive current control technique is developed and its advantages over the other types of current control techniques are comparatively discussed. The aim of the current control is for the phase current to exactly follow the desired current reference with a minimum current ripple and phase delay.

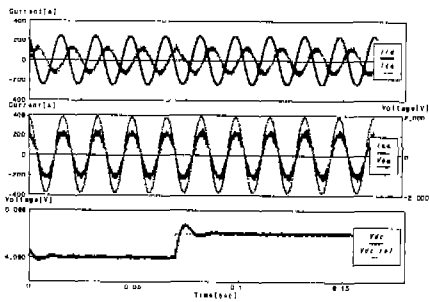


Fig. 14 Transient responses of hysteresis current control when DC link voltage reference is changed (4000V→5000V) at $t=0.07\text{sec}$

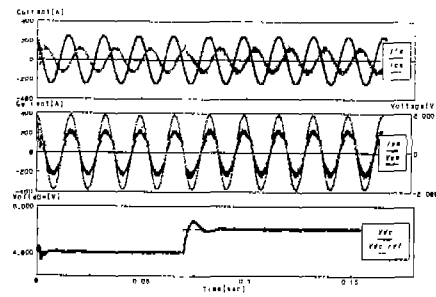


Fig. 16 Transient responses of PI with ramp comparison current control when DC link voltage reference is changed (4000V→5000V) at $t=0.07\text{sec}$

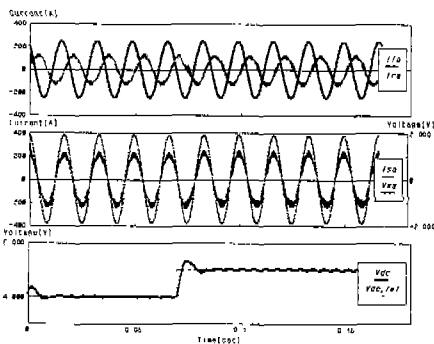


Fig. 15 Transient responses of ramp comparison current control when DC link voltage reference is changed (4000V→5000V) at $t=0.07\text{sec}$

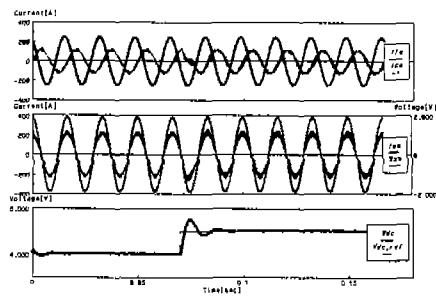


Fig. 17 Transient responses of predictive current control when DC link voltage reference is changed (4000V→5000V) at $t=0.07\text{sec}$

The simple block diagrams of the various current controller and space vector predictive current controller are shown in Fig. 5 and Fig. 6, respectively [13]. The signal flow diagram in Fig. 5(a) shows three hysteresis controllers. Each controller determine the switching-state of one inverter leg such that the error of the corresponding phase current is maintained within the hysteresis band. The major advantage of this control is simple implementation, and its dynamic performance is excellent. However, there are some inherent drawbacks such as no intercommunication between the individual hysteresis controller and varied switching frequency. The constant switching frequency PWM can be easily obtained by a so-called ramp comparison modulator. The signal flow diagram in Fig. 5(b) shows three ramp comparison controllers. A triangular waveform signal at the desired switching is used to provide the ramp and the phase current error

forms the ramp comparison. The comparator output directly determines the inverter switching. However, the ramp comparison control shows some the steady-state error and phase delay. Fig. 5(c) shows the signal flow diagram of the PI current control with ramp comparison. A PI controller is commonly used to provide a high DC gain, which eliminate steady-state errors and provides a controlled roll-off of the high frequency response. However, the dynamic responses are always depends on the PI controller and it shows the slow transient characteristic which may results in the uncontrollability of the DC link voltage in transient region.

The overall block diagram of a space vector predictive current controller is shown in Fig. 6. By using the circuit information in the present sampling period, the compensation current trajectory in next sampling period is predicted.

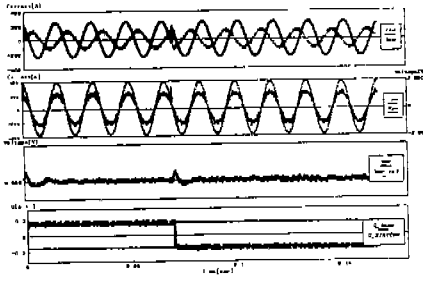


Fig. 18 Transient responses of hysteresis current control when load is changed (capacitive→inductive) at t=0.07sec

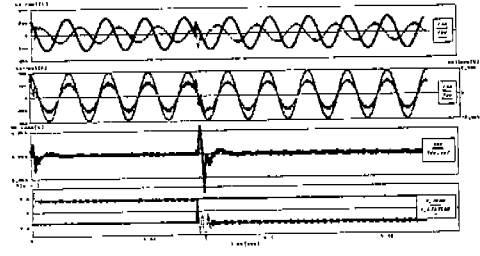


Fig. 20 Transient responses of PI with ramp comparison current control when load is changed (capacitive→inductive) at t=0.07sec

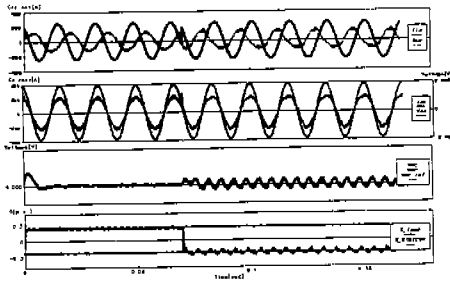


Fig. 19 Transient responses of ramp comparison current control when load is changed (capacitive→inductive) at t=0.07sec

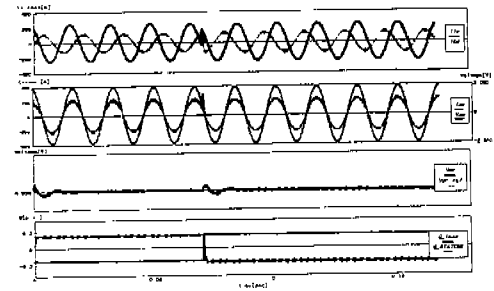


Fig. 21 Transient responses of predictive current control when load is changed (capacitive→inductive) at t=0.07sec

Therefore, the inverter switching function can be determined, which forces the compensation current to follow the current reference. The error of the dc link voltage is controlled by a PI controller. The output of the PI controller is used as the magnitude of the current reference. The current reference is sent to calculate the required reference voltage which forces the compensation current to be in phase with source voltage in case of unity power factor. Knowing the reference voltage and the modulation strategy, it is possible to calculate the necessary duty-cycles. In this scheme, the space vector modulation is employed. From (2), the voltage equation can be written as follows:

$$V_{Oqe} = -L \frac{di_{qe}}{dt} - R_s i_{qe} - \omega i_{de} + V_{Sqe} \quad (3)$$

$$V_{Ode} = -L \frac{di_{de}}{dt} - R_s i_{de} + \omega i_{qe} + V_{Sde} \quad (4)$$

where V_{Oqe} and V_{Ode} represent DQ transformed inverter output voltage. The required reference voltage which make the current errors at (k+1)-th sampling time instant zero can be obtained in the discrete form as follows:

$$V_{cqe}(k) = -L \frac{[i_{qe,ref}(k+1) - i_{qe}(k)]}{T_s} - R_s i_{qe}(k) - \omega i_{de}(k) + V_{Sqe}(k) \quad (5)$$

$$V_{cde}(k) = L \frac{[i_{de,ref}(k+1) - i_{de}(k)]}{T_s} - R_s i_{de}(k) + \omega i_{qe}(k) + V_{Sde}(k) \quad (6)$$

where T_s is a sampling time, and $i_{qe,ref}(k+1)$ and $i_{de,ref}(k+1)$ are the q-axis and d-axis current references at (k+1)-th instant, respectively. The computed reference voltage vector $V_{c,ref}$ is applied to D-STATCON using the space vector PWM technique. Based on this technique, the conduction periods of the inverter switches are modulated according to the amplitude and angle of the

reference voltage vector to obtain the average voltage equal to the reference. Fig. 7 shows the computation example of the space vector PWM technique. In this figure, the time durations of V1, V3, and the zero voltage vector are given by

$$t_A = \frac{\sqrt{3} |V_{c,ref}|}{V_{dc}} \sin\left(\frac{\pi}{3} - \delta\right) \cdot T_s \quad (6)$$

$$t_B = \frac{\sqrt{3} |V_{c,ref}|}{V_{dc}} \sin \delta \cdot T_s \quad (7)$$

$$t_Z = T_s - (t_A + t_B) \quad (8)$$

where V_{dc} is a dc link voltage. Also $|V_{c,ref}|$ and δ are given as

$$|V_{c,ref}| = \sqrt{V_{cqe,ref}^2 + V_{cde,ref}^2} \quad (9)$$

$$\delta = \theta - \tan^{-1}\left(\frac{V_{cqe,ref}}{V_{cde,ref}}\right) \quad (10)$$

IV. COMPARATIVE SIMULATION RESULTS

The computer simulations are made for the measurements of the rectifier steady-state performance and dynamic response of the predictive current control technique with other types of current control techniques such as hysteresis, ramp comparison and PI with ramp comparison current controller at the effect of the small dc link filter capacitor on the current and voltage ripple as well as the transient response. Fig. 9-13 shows the comparative simulation results for the hysteresis, ramp comparison, PI with ramp comparison, and predictive current control schemes. The parameter used in this simulation are as follows

$$\begin{aligned} V_{Sab} &= 3.3kV_{rms}, & L &= 4.2mH, & R_s &= 0.4 \Omega, \\ C &= 100 \mu F, & f_s &= 3kHz, & V_{dc,ref} &= 4000V. \end{aligned}$$

In this simulation, the control performance of Fig. 9 and 10 are generally shown to be undesirable with respect to current ripple and offset. It is difficult to obtain an optimized response in the sense of reduced current ripple and offset. As can be seen in this figure, the PI with ramp comparison, and predictive current control technique show a better performance compared

with the other control techniques, with respect to the line current harmonics. Fig. 13 shows the q-d current reference and current of predictive current control technique. Fig. 14-17 shows the transient responses of hysteresis, ramp comparison, PI with ramp comparison, and predictive current control technique when the DC link voltage reference is changed at 0.07 sec. As can be seen in this figure, all controller shows similar responses of DC link voltage. Fig. 18-21 shows the transient responses of hysteresis, ramp comparison, PI with ramp comparison, and predictive current control technique for step change in the load from capacitive to inductive at 0.07 sec. In these figures, the ramp comparison current control technique shows the undesirable DC link voltage oscillation and PI with ramp comparison current controller shows the undesirable transient response of DC link voltage and line current compared with the predictive current controller due to the employing the PI current regulator. In case of predictive control, a fast dynamic response can be obtain without current oscillations. Thus, it can be considered that the proposed DQ modeling and predictive current control technique are very useful for the power factor correction of three-phase rectifier with low line current harmonics and reduced size of the harmonic filter.

V. CONCLUSIONS

The modeling and space vector predictive current control for use in D-STATCON has been presented in this paper. The space vector predictive current control is accomplished by calculating the duration of time spent on the appropriate inverter states in order to drive D-STATCON compensation current to the reference value at the end of the cycle. This controller shows the better control performances in lower harmonic current distortion and fast transient responses in comparison with existing current controller.

VI. REFERENCES

- [1] H. Mehta, T.W. Cease, L. Gyugyi, and C.D. Schauder, "Static condenser for flexible AC transmission system," FACTS EPRI Workshop, May. 1992.
- [2] J.P. Kessinger, "The feasibility of FACTS." International Conference on Electricity Delivery & Power Quality, pp. 1-13, Nov. 1996.
- [3] J.P. Kessinger, "Advanced power electronics as an enabler of unbundled power quality services," NSF Conference on Unbundled Power Quality Services, pp. 1-7, Nov. 1996.
- [4] S.A. Waples and A.S. Law, "Planning and operating ratings for inverter-based FACTS power flow controller," The American Power Conference, April 1996.
- [5] I.A. Erinmez, Ed, "Static Var compensator " Working Group 38-01, Task force NO. 2.
- [6] L. Gyugui, "Reactive power generation and control by thyristor circuits," IEEE Trans. IA, vol. IA-15, no. 5, pp. 521-532, Sept, 1979.
- [7] Guk C. Cho, Gu H. Jung, Nam S. Choi, and Gyu H. Cho, " Analysis and controller design of static var compensator using three-level GTO inverter," IEEE Trans. Power Electronics, vol. 11, NO. 1, pp. 57-65, Jan. 1996.
- [8] Habetler, T.G. and Divan, D.M., " Angle Controlled Current Regulated Rectifier for AC/AC Converter," IEEE PESC, pp. 704-710, June. 1989.
- [9] R. Wu, S.B. Dewan, and G.R. Slemon, " A PWM AC to DC Converter with Fixed Switching Frequency", IEEE IAS Annual Meeting Conference Record, 1988, pp. 706-711.
- [10] G. Joos, L. Moran, and P.D. Ziogas, "Performance analysis of a PWM inverter VAR compensator," IEEE Trans. Power Electronics, vol. 6, NO. 6, pp. 380-391, July 1991.
- [11] H.A. Kojori, S.B. Dewan, and J.D. Lavers, "A large-scale PWM solid-state synchronous condenser," IEEE Trans. Ind. Applicat., vol. 6, NO. 1, pp. 41-49, Jan/Feb. 1992.
- [12] Chun T. Rim, Nam S. Choi, Guk C. Cho, and Gyu H. Cho, "A complete dc and ac analysis of three-phase controlled-current PWM rectifier using circuit dq transformation," IEEE Trans. Power Electronics, vol. 9, NO. 4, pp. 390-396, July 1994.
- [13] Bimal K. Boss, "Power electronics and variable frequency drives," IEEE Press, 1997.